Generation of a frequency comb of squeezing in an optical parametric oscillator

A. E. Dunlop and E. H. Huntington
Centre for Quantum Computer Technology, School of Information Technology and Electrical Engineering, University College, The University of New South Wales, Canberra, ACT 2600, Australia

C. C. Harb
Centre for Quantum-Atom Optics, Faculty of Science, The Australian National University, Canberra, ACT 0200, Australia

T. C. Ralph
Centre for Quantum Computer Technology, Department of Physics, The University of Queensland, St. Lucia, QLD 4072, Australia
(Received 16 September 2005; published 26 January 2006)

The multimode operation of an optical parametric oscillator (OPO) operating below threshold is calculated. We predict that squeezing can be generated in a comb that is limited only by the phase matching bandwidth of the OPO. Effects of technical noise on the squeezing spectrum are investigated. It is shown that maximal squeezing can be obtained at high frequency even in the presence of seed laser noise and cavity length fluctuations. Furthermore the spectrum obtained by detuning the laser frequency off OPO cavity resonance is calculated.

DOI: 10.1103/PhysRevA.73.013817 PACS number(s): 42.50.Lc

I. INTRODUCTION

Squeezed light displays quadrature fluctuations that are less than the quantum noise limit (QNL) set by the quadrature fluctuations of the vacuum [1]. No classical theory can consistently explain the appearance of such sub-QNL fluctuations. Applications for squeezed light have been identified in communications, gravitational wave detection, and various quantum information tasks [2]. While a basic understanding of the physics can be obtained from a single mode theory, a detailed understanding of squeezing phenomena requires a multimode theory. Considerable attention has been paid in recent years to the understanding and control of multimode squeezed light in terms of both spatial [3,4] and frequency modes [5,6].

Squeezing is typically produced by a cavity enhanced nonlinear interaction. When squeezing spectra are calculated and measured, only frequencies within a single cavity bandwidth are normally considered. The focus of this work is on the dynamics of cavity enhanced squeezing in which multiple longitudinal modes are considered. Though squeezing at higher longitudinal modes has been seen in four-wave-mixing systems [7] and derived for optical parametric oscillators (OPOs) [8], we generalize the description of the OPO to include cavity detuning and consider experimental implications to the squeezing spectrum at frequencies corresponding to higher longitudinal cavity modes.

In Sec. II, we present a quantum mechanical derivation of the output of a singly resonant subthreshold OPO where many longitudinal cavity modes are considered. Then, in Sec. III we show that squeezing may be obtained at sideband frequencies corresponding to the free-spectral range (FSP) of the OPO cavity. The effects of seeding, technical noise, cavity length fluctuations, and detuning on the multimode OPO are also discussed in this section. We conclude in Sec. IV.

II. MULTIMODE THEORY

Figure 1(a) illustrates the standard approach to generating squeezing from a subthreshold OPO [9]. A laser operating at the "fundamental" frequency undergoes frequency doubling in a second harmonic generator (SHG), the output of which is then used to pump an OPO. A fraction of the fundamental is tapped off prior to the SHG to serve as a local oscillator

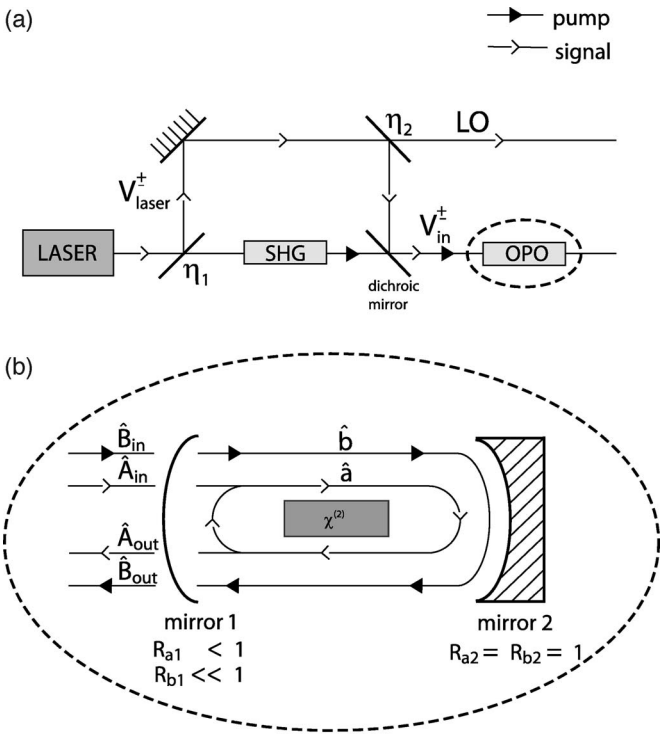

FIG. 1. Schematic of quadrature squeezing system. (a) Overall system where η_1 and η_2 are beamsplitter reflectivities. (b) Detailed schematic of OPO.

(LO) for subsequent homodyne measurements [2]. The tap off may also be used as a seed for the subthreshold OPO. Focusing now on the OPO as the nonclassical light source, the interaction Hamiltonian for parametric downconversion is [10]

$$H = i\hbar\chi^{(2)}(\hat{b}^\dagger\hat{a}^2 - \hat{a}^{\dagger 2}\hat{b}), \tag{1}$$

where $\hat{a}$ and $\hat{b}$ are the annihilation operators for the intracavity fundamental and second harmonic modes, respectively. The nonlinear crystal's second order coefficient of nonlinearity is given by $\chi^{(2)}$, and we have assumed the crystal phase matching bandwidth to be very broad compared to the frequencies of interest and have thus taken it to be infinite. As illustrated in Fig. 1(b), we consider a singly resonant, degenerate configuration where only the fundamental photons resonate inside a single ended, lossless cavity. Under these conditions and assuming that the pump field is undepleted, the Hamiltonian Eq. (1) can be approximated [1]

$$H = \frac{i\hbar\chi}{2}(\hat{a}^2 - \hat{a}^{\dagger 2}), \tag{2}$$

where $\chi = 2\chi^{(2)}\beta_{in}$ and β_{in} (taken to be real without loss of generality) is the amplitude of the pump field. Following the approach of Ref. [2], the fundamental cavity mode $\hat{a}$ after a single cavity round trip can be written

$$\hat{a}(t+\tau) = e^{i\Delta\tau}[-\chi\tau\hat{a}^\dagger(t) + (1-\kappa_a\tau)\hat{a}(t) + \sqrt{2\kappa_a}\tau\hat{A}_{in}(t)], \tag{3}$$

where the cavity decay rate for the fundamental mode is determined by the mirror reflectivity R_a and is given by $\kappa_a = (1-R_a)/2\tau$ for a cavity round trip time of τ. The field incident on the front face of the cavity at the fundamental is given by $\hat{A}_{in}$. The detuning between the fundamental and the cavity resonant frequency is Δ.

It is convenient to decompose the field operators in the form $\hat{a} = \langle\hat{a}\rangle + \delta\hat{a}$. In the steady state, we have $\langle\hat{a}(t+\tau)\rangle = \langle\hat{a}(t)\rangle$ and thus, from Eq. (3) the steady state solution for the expectation value of the field amplitude is given by

$$\alpha = \langle\hat{a}\rangle = \frac{\sqrt{2\kappa_a}\left(\kappa_a - \dfrac{1-e^{i\Delta\tau}}{\tau} - \chi\right)}{\left(\kappa_a - \dfrac{1-e^{i\Delta\tau}}{\tau}\right)\left(\kappa_a - \dfrac{1-e^{-i\Delta\tau}}{\tau}\right) - \chi^2}\alpha_{in}. \tag{4}$$

In steady state the operator fluctuations obey

$$\delta\hat{a}(t+\tau) = e^{i\Delta\tau}[-\chi\tau\delta\hat{a}^\dagger(t) + (1-\kappa_a\tau)\delta\hat{a}(t) + \sqrt{2\kappa_a}\tau\delta\hat{A}_{in}(t)]. \tag{5}$$

Equtation (5) is straightforward to solve in the frequency domain. The Fourier transform of the left side of Eq. (5) is

$$\delta\hat{a}(t+\tau) \rightleftharpoons \delta\tilde{a}(\omega)e^{i\omega\tau}, \tag{6}$$

where the tilde rather than a caret is used to indicate operators in the frequency domain. Solving for the fluctuating part of the cavity mode in the frequency domain, we obtain

$$\delta\tilde{a}(\omega) = \frac{-\chi\delta\tilde{a}(\omega)^\dagger + \sqrt{2\kappa_a}\delta\tilde{A}_{in}(\omega)}{\kappa_a - \dfrac{1-e^{i(\omega-\Delta)\tau}}{\tau}}. \tag{7}$$

The output operator $\tilde{A}_{out} = \sqrt{2\kappa_a}\tilde{a} - \tilde{A}_{in}$ [12] and so

$$\delta\tilde{A}_{out}(\omega) = \frac{\left[\left(\kappa_a - \dfrac{1-e^{i(\omega+\Delta)\tau}}{\tau}\right)\left(\kappa_a + \dfrac{1-e^{i(\omega-\Delta)\tau}}{\tau}\right) + \chi^2\right]\delta\tilde{A}_{in}(\omega) - 2\kappa_a\chi\delta\tilde{A}_{in}(-\omega)^\dagger}{\left(\kappa_a - \dfrac{1-e^{i(\omega+\Delta)\tau}}{\tau}\right)\left(\kappa_a - \dfrac{1-e^{i(\omega-\Delta)\tau}}{\tau}\right) - \chi^2}, \tag{8}$$

$$\delta\tilde{A}_{out}(-\omega)^\dagger = \frac{\left[\left(\kappa_a + \dfrac{1-e^{i(\omega+\Delta)\tau}}{\tau}\right)\left(\kappa_a - \dfrac{1-e^{i(\omega-\Delta)\tau}}{\tau}\right) + \chi^2\right]\delta\tilde{A}_{in}(-\omega)^\dagger - 2\kappa_a\chi\delta\tilde{A}_{in}(\omega)}{\left(\kappa_a - \dfrac{1-e^{i(\omega+\Delta)\tau}}{\tau}\right)\left(\kappa_a - \dfrac{1-e^{i(\omega-\Delta)\tau}}{\tau}\right) - \chi^2}. \tag{9}$$

To obtain this result we have used that $\delta\tilde{a}^\dagger(\omega) = \delta\tilde{a}(-\omega)^\dagger$ [11].

Equations (8) and (9) describe the dynamics of the OPO at Fourier frequencies far beyond those normally considered for these types of systems. This multiple longitudinal mode description is a generalization of the standard result for an OPO, allowing consideration of the squeezing spectrum of the OPO out to many free spectral ranges (FSRs) of the cavity. If $\Delta = 0$ and we look only at frequencies much less than the free spectral range (FSR), Eqs. (8) and (9) reduce to the standard equations for an OPO [2].

The coherent amplitude acquires a phase shift of

$$\tan\phi_{out} = \frac{\frac{2\kappa_a}{\tau}\sin(\Delta\tau)}{(\kappa_a-\chi)^2 - \frac{2}{\tau^2}[1-\cos(\Delta\tau)]}, \tag{10}$$

upon reflection from a detuned cavity. Taking this phase shift into account, amplitude and phase quadratures fluctuations are defined in the frequency domain as

$$\delta\tilde{X}^+(\omega) = \delta\tilde{A}(\omega)e^{-i\phi_{out}} + \delta\tilde{A}(-\omega)^\dagger e^{i\phi_{out}}, \tag{11}$$

$$\delta\tilde{X}^-(\omega) = i[\delta\tilde{A}(\omega)e^{-i\phi_{out}} - \delta\tilde{A}(-\omega)^\dagger e^{i\phi_{out}}], \tag{12}$$

respectively, which lead to the amplitude and phase quadrature variances $V^\pm(\omega)=\langle|\delta\tilde{X}^\pm(\omega)|^2\rangle$ and thus

$$V^+_{out}(\omega) = \frac{1}{\left|\left(\kappa_a - \frac{1-e^{i(\omega+\Delta)\tau}}{\tau}\right)\left(\kappa_a - \frac{1-e^{i(\omega-\Delta)\tau}}{\tau}\right) - \chi^2\right|^2}\left[\left(\left|(\kappa_a+\chi)^2 - \frac{1-e^{i(\omega+\Delta)\tau}}{\tau}\frac{1-e^{i(\omega-\Delta)\tau}}{\tau}\right|^2\cos^2\phi_{out} + \frac{4\kappa_a^2}{\tau^2}\sin^2(\Delta\tau)\sin^2\phi_{out}\right)V^+_{in}(\omega) - \left(\left|(\kappa_a-\chi)^2 - \frac{1-e^{i(\omega+\Delta)\tau}}{\tau}\frac{1-e^{i(\omega-\Delta)\tau}}{\tau}\right|^2\sin^2\phi_{out} - \frac{4\kappa_a^2}{\tau^2}\sin^2(\Delta\tau)\cos^2\phi_{out}\right)V^-_{in}(\omega)\right], \tag{13}$$

$$V^-_{out}(\omega) = \frac{1}{\left|\left(\kappa_a - \frac{1-e^{i(\omega+\Delta)\tau}}{\tau}\right)\left(\kappa_a - \frac{1-e^{i(\omega-\Delta)\tau}}{\tau}\right) - \chi^2\right|^2}\left[\left(\left|(\kappa_a+\chi)^2 - \frac{1-e^{i(\omega+\Delta)\tau}}{\tau}\frac{1-e^{i(\omega-\Delta)\tau}}{\tau}\right|^2\sin^2\phi_{out} + \frac{4\kappa_a^2}{\tau^2}\sin^2(\Delta\tau)\cos^2\phi_{out}\right)V^+_{in}(\omega) + \left(\left|(\kappa_a-\chi)^2 - \frac{1-e^{i(\omega+\Delta)\tau}}{\tau}\frac{1-e^{i(\omega-\Delta)\tau}}{\tau}\right|^2\cos^2\phi_{out} + \frac{4\kappa_a^2}{\tau^2}\sin^2(\Delta\tau)\sin^2\phi_{out}\right)V^-_{in}(\omega)\right]. \tag{14}$$

When the cavity is resonant with the OPO seed, the output variances greatly simplify to

$$V^\pm_{out}(\omega) = \left|\frac{(\kappa_a\pm\chi)^2 - \left(\frac{1-e^{i\omega\tau}}{\tau}\right)^2}{\left(\kappa_a - \frac{1-e^{i\omega\tau}}{\tau}\right)^2 - \chi^2}\right|^2 V^\pm_{in}(\omega). \tag{15}$$

Note that Eqs. (13)–(15) show resonant behavior at $2\pi n = (\omega+\Delta)\tau$ where n is an integer.

III. DISCUSSION

Let us first consider the best possible output which could be produced with a classical seed. This occurs when the cavity is resonant with the OPO seed and when the OPO seed is at the QNL in both quadratures, i.e., $V^+_{in}(\omega)=V^-_{in}(\omega)=1$. Figure 2 is a plot of the variance of the phase quadrature $V^-_{out}(\omega)$ under these conditions. This plot was generated assuming $\Delta=0$ GHz, FSR=10 GHz, $R_A=0.95$, and $\chi/\chi_{threshold}=0.15$. Unless stated otherwise, these parameters were used to generate all of the figures in this paper.

Figure 2 shows that squeezing is produced at low Fourier frequencies as expected and also at every subsequent resonance of the OPO cavity. As a consequence, a comb of squeezing is generated with the frequency spacing given by the cavity FSR. The squeezing spectrum follows the line shape of the OPO cavity. Note that the maximum squeezing is the same at each resonance. The total number of modes will be governed by the phase matching bandwidth of the nonlinear system.

In experiments, there are sources of technical noise which have been ignored in order to generate Fig. 2. We will now examine the effects of two of the main sources of technical noise: optical noise carried by a non-QNL seed and noise introduced by fluctuations of the length of the OPO cavity.

To model optical noise carried by the seed, we treat the seed as an attenuated laser as shown in Fig. 1. The amount of seed entering the OPO cavity is determined by the reflectivities of the beam splitters (η_1 and η_2) and expressed as the ratio $|\alpha_{in}/\beta_{in}|^2$. We set $V^+_{laser}(\omega)=1$, $V^-_{laser}(\omega)=1+|1000/\omega|$, and $V^\pm_{in}=\eta_1\eta_2 V^\pm_{laser}+(1-\eta_1\eta_2)$. Here we assume the laser is quantum noise limited in the amplitude quadrature and we approximate the quadrature phase noise spectrum of the laser as "$1/f$" noise. Figure 3(a) is a plot of V^-_{out} as a function of sideband frequency on a logarithmic scale, where for clarity we have assumed there are no fluctuations in the length of the OPO cavity. Figure 3(a) shows that squeezing is seen at multiple cavity modes and because the technical seed noise is greater at lower frequencies, the amount of squeezing is greatest at resonant frequencies distant from the degenerate downconversion frequency, i.e., $\omega/\mathrm{FSR}\gg 0$. The low fre-

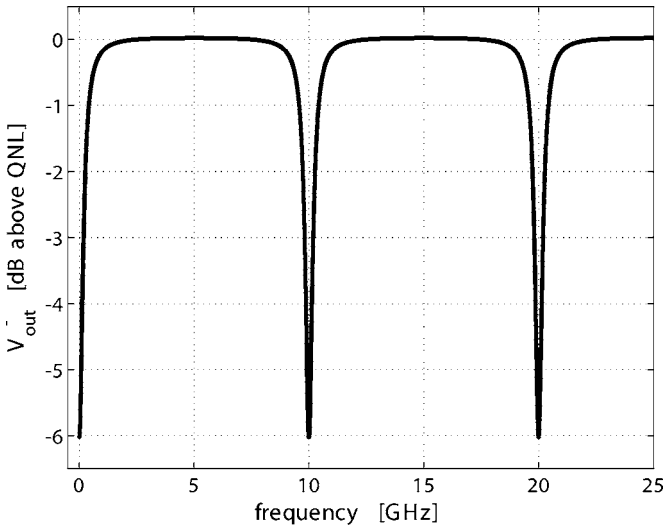

FIG. 2. Variance of the phase quadrature in an OPO.

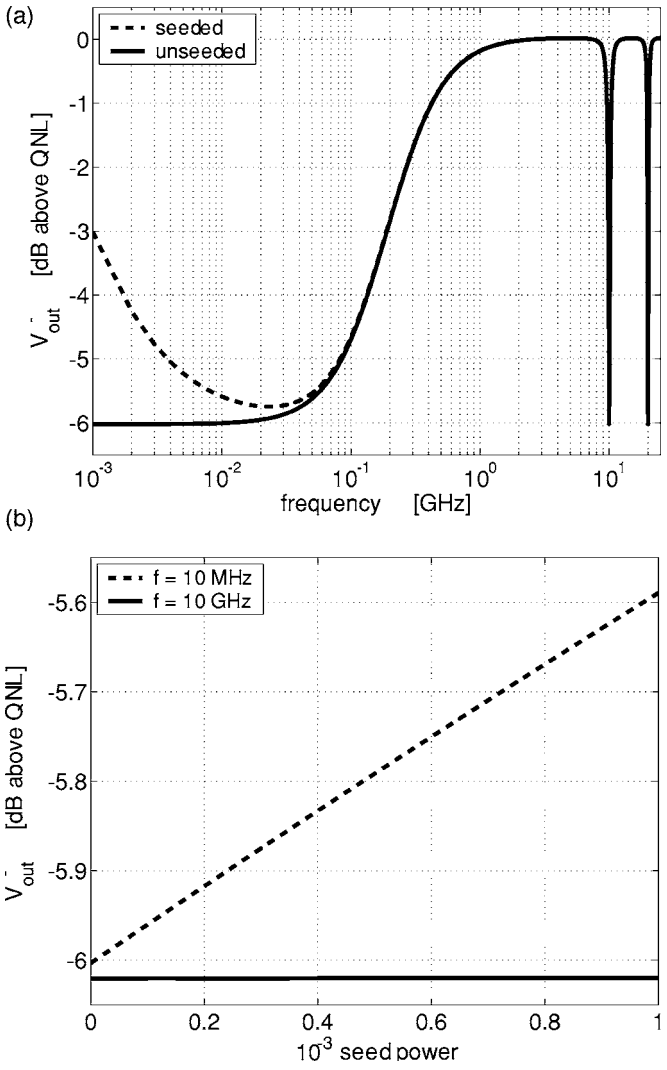

FIG. 3. Phase quadrature squeezing of a seeded OPO: (a) As a function of frequency with seed power $|\alpha_{in}/\beta_{in}|^2=10^{-3}$ (broken line) and 0 (continuous line). (b) As a function of seed power at f=10 MHz (broken line) and 10 GHz (continuous line).

quency noise introduced into the OPO by the seed scales linearly with seed power, and hence great effort at running a genuinely seedless OPO has led to improvements in squeezing at frequencies in the sub-kHz range [13]. However, Fig. 3(a) shows that because the noise introduced by the seed is at the QNL at high frequencies, the seed does not affect the magnitude of squeezing at the higher cavity resonances. Figure 3(b) illustrates that the squeezing at the higher cavity resonances is fairly independent of the seed power, whereas the squeezing at low frequencies degrades with increased seed power.

Cavity length fluctuations are incorporated into the model by setting $\Delta=\bar{\Delta}+\delta\Delta(t)$ where $\bar{\Delta}$ represents the average detuning and $\delta\Delta(t)$ represents time varying fluctuations. This decomposition of Δ is substituted into Eq. (3) and the approach outlined in Sec. II is followed where terms are only retained to first order, i.e., we assume that $\delta\Delta \ll \bar{\Delta}$ and make the approximation that terms such as $\delta\Delta\,\delta a \approx 0$. The output quadrature amplitude and phase variances are as given in Eqs. (13) and (14) where Δ is replaced with $\bar{\Delta}$ and additional noise terms arise. The full expression for these noise terms is relatively straightforward to calculate but the resulting equations are unwieldy and not particularly revealing of the underlying physics. For the specific, experimentally realistic case of $\bar{\Delta}=0$, the output quadrature variances are

$$V_{out}^{+}(\omega)=\left|\frac{(\kappa_a+\chi)^2-\left(\frac{1-e^{i\omega\tau}}{\tau}\right)^2}{\left(\kappa_a-\frac{1-e^{i\omega\tau}}{\tau}\right)^2-\chi^2}\right|^2 V_{in}^{+}(\omega), \tag{16}$$

$$V_{out}^{-}(\omega)=\left|\frac{(\kappa_a-\chi)^2-\left(\frac{1-e^{i\omega\tau}}{\tau}\right)^2}{\left(\kappa_a-\frac{1-e^{i\omega\tau}}{\tau}\right)^2-\chi^2}\right|^2 V_{in}^{-}(\omega)+\frac{16\kappa_a^2\left[\frac{\kappa_a}{\tau}-\chi(\chi+\kappa_a)\right]^2}{(\kappa_a^2-\chi^2)^2}\left|\frac{\kappa_a+\chi-\frac{1-e^{i\omega\tau}}{\tau}}{\left(\kappa_a-\frac{1-e^{i\omega\tau}}{\tau}\right)^2-\chi^2}\right|^2 \alpha_{in}^2 V_{\Delta}(\omega), \tag{17}$$

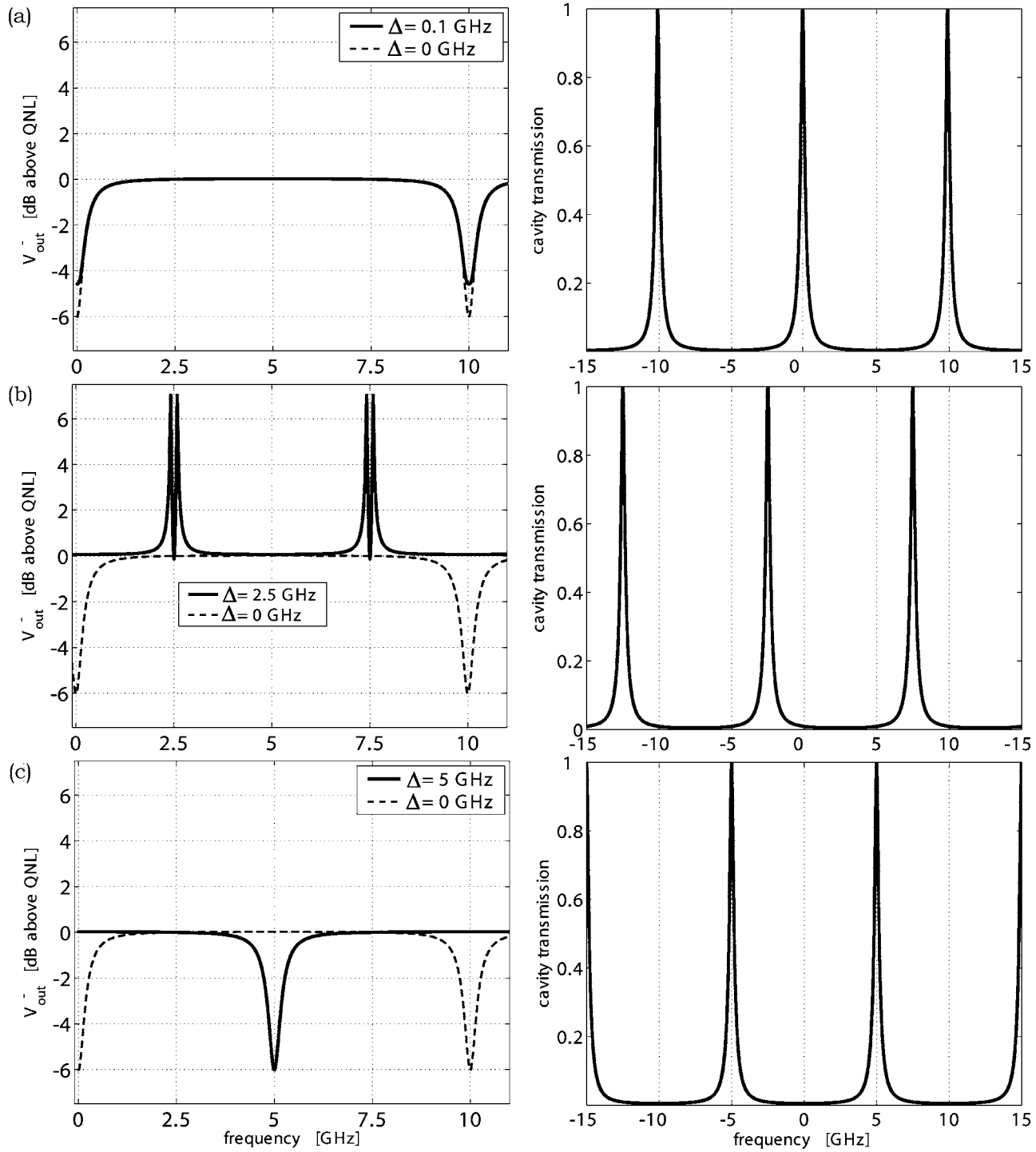

FIG. 4. Variance of the phase quadrature (left column) and cavity transmission (right column) in an OPO with Δ=(a) 0.1 GHz, (b) 2.5 GHz, and (c) 5 GHz.

where $V_\Delta(\omega)=\langle \delta l(\omega)^2\rangle/L^2$ represents the noise spectrum due to cavity length fluctuations. Here $\delta l(\omega)$ is the Fourier spectrum of the OPO cavity length fluctuations and L is the average OPO cavity length.

Physically, cavity length fluctuations impose a classical phase modulation onto the output of the OPO. The magnitude of this phase modulation relative to the QNL scales with the intracavity field amplitude. Hence, to first order, a genuinely seedless OPO would be immune to technical noise arising from cavity length fluctuations. While the transfer of cavity length fluctuations to the OPO output is strongest at each of the resonances of the OPO cavity, mechanical length fluctuations are typically "slow" and so would have a much more deleterious effect on the squeezing at low frequencies than at higher frequencies. Therefore, much like the case for technical noise introduced by the optical seed to the OPO, stronger squeezing will be seen at high cavity resonances.

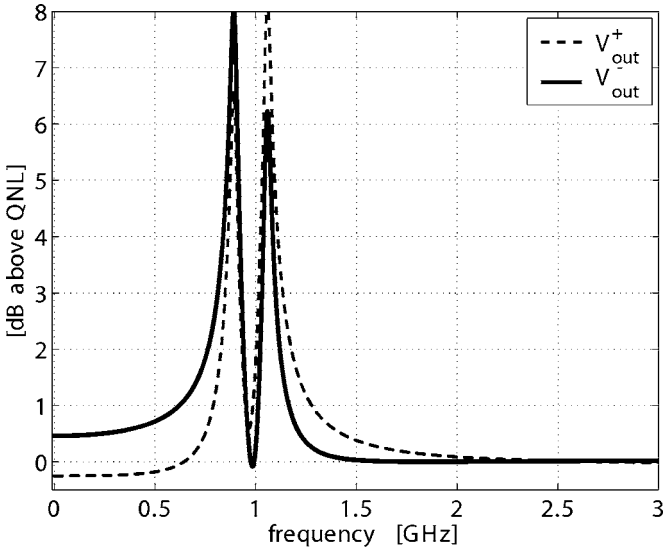

FIG. 5. Phase and amplitude quadrature variances for $\Delta=1$ GHz.

Measurements of variances probe the power of and the correlation between the positive and negative sidebands of a field. It is possible to alter both the relative magnitudes and phases of the sidebands of the downconverted field by detuning the OPO cavity resonance away from the laser frequency, i.e., setting $\Delta \neq 0$. This can result in unusual squeezing spectra as shown in Fig. 4. When the laser frequency is detuned from the OPO cavity resonance, the cavity transmission may not be the same for both the positive and negative frequency sidebands and this could lead to decreased squeezing on the output. This is illustrated in Fig. 4(a) where the squeezing spectrum is plotted for $\Delta=0.1$ GHz. For reference, the squeezing spectrum for $\Delta=0$ is also shown in this figure. In Fig. 4(b), $\Delta=2.5$ GHz and no squeezing is observed as there is effectively only one sideband escaping the OPO cavity. For illustration, the transmission function of the OPO cavity as a function of frequency relative to the carrier is plotted in the right hand column of Fig. 4.

When the laser is tuned to be exactly half-way between two OPO cavity resonances, the full squeezing of the OPO is restored. This is shown in Fig. 4(c), where $\Delta=5$ GHz. This occurs because the transmission spectrum of the OPO cavity is again symmetric about the laser frequency as sketched on the right of Fig. 4(c). The squeezing is maximized at $\omega=\mathrm{FSR}/2$ because this is the frequency for which generation of the correlated sideband pairs is maximized. In contrast to the case when $\Delta=0$, squeezing cannot be seen near $\omega=0$. This is because the OPO cavity does not support the generation of sidebands near the laser frequency.

Finally, interesting effects can result from the phase shift acquired across a cavity resonance. Figure 5 shows the output spectra for both the amplitude and phase quadratures of an OPO with $\Delta=1$ GHz. The plots clearly illustrate the result when positive and negative sidebands emerge from an OPO with different amplitudes and different phases. Here we see that the phase quadrature noise is enhanced above the QNL at low frequencies while the opposite occurs for the amplitude quadrature. This is different to the general case for $\Delta=0$ GHz where squeezing is in the phase quadrature and antisqueezing in the amplitude quadrature. At $\Delta=0$, the positive and negative sidebands show perfect phase antisymmetry at all frequencies due to the antisymmetric phase shift across the cavity. However when $\Delta \neq 0$, the upper and lower sidebands can acquire different phase shifts resulting in frequency dependent rotation of the squeezing ellipse [14]. Indeed, as seen in Fig. 5, the phase quadrature spectrum maps the phase response of the OPO cavity at high frequencies. Measurements of the amplitude and phase quadrature variances of a rotated squeezing ellipse result in $V^+_{out}V^-_{out}>1$. Hence another effect of the phase shift acquired across the OPO cavity is that $V^+_{out}V^-_{out}$ will be strongly frequency dependent. This is illustrated in Fig. 6 where V^+_{out}, V^-_{out}, and $V^+_{out}V^-_{out}$ are plotted for $\Delta=0$ GHz and 0.1 GHz.

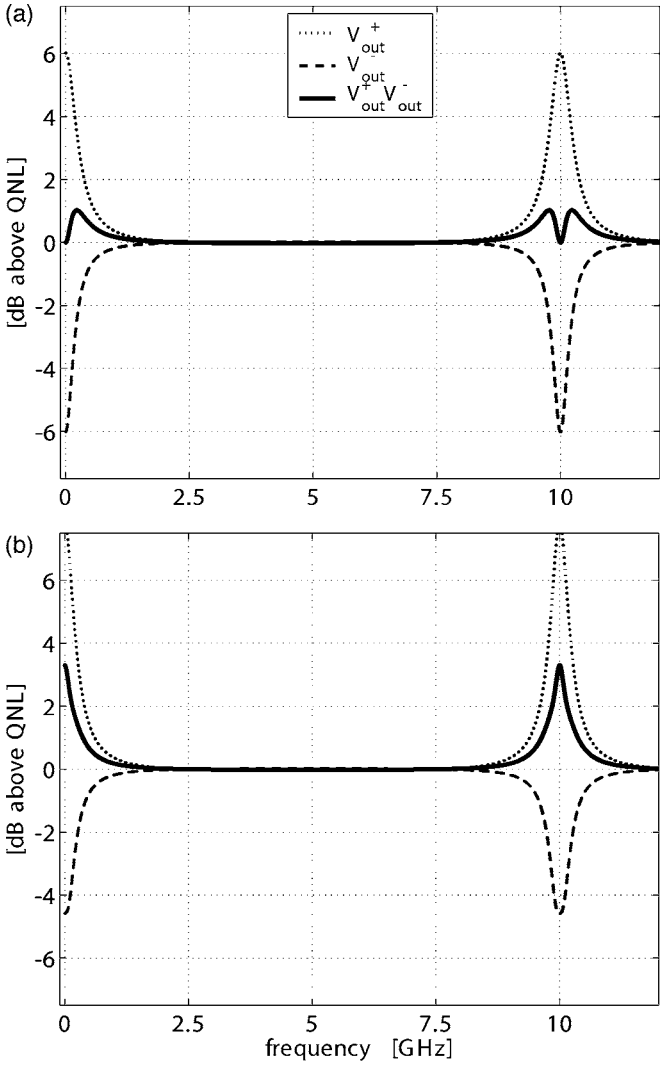

FIG. 6. Phase quadrature, amplitude quadrature, and total quadrature variances with $\Delta=$(a) 0 GHz and (b) 0.1 GHz.

IV. CONCLUSION

An OPO operating below threshold generates correlated pairs of photons that are emitted into multiple frequency

modes of the OPO cavity. As a consequence of this, a subthreshold OPO can generate a comb of squeezing in the frequency domain with the spacing determined by the cavity FSR. In the ideal case, the squeezing seen at all resonances is identical, however in practice the greatest amount of squeezing is expected at higher frequencies. This is because technical noise from the OPO seed and from cavity length fluctuations is greatest at low frequencies. Unusual squeezing spectra can be generated when the source laser is detuned from resonance with the OPO cavity.

ACKNOWLEDGMENTS

T.C.R. wishes to thank Franco Wong for motivating discussions. This research was supported by the Australian Research Council.

[1] D. F. Walls and G. J. Milburn, *Quantum Optics* (Springer-Verlag, Berlin, 1994).
[2] H.-A. Bachor and T. C. Ralph, *A Guide To Experiments In Quantum Optics*, 2nd ed. (Wiley-VCH, Berlin, 2003).
[3] N. Treps, N. Grosse, W. P. Bowen, C. Fabre, H.-A. Bachor, and P. K. Lam, Science **301**, 940 (2003).
[4] L. Lopez, S. Gigan, N. Treps, A. Maître, C. Fabre, and A. Gatti, Phys. Rev. A **72**, 013806 (2005).
[5] S. Inoue, S. Lathi, and Y. Yamamoto, J. Opt. Soc. Am. B **14**, 2761 (1997).
[6] E. H. Huntington, G. N. Milford, C. Robilliard, T. C. Ralph, O. Glöckl, U. L. Andersen, S. Lorenz, and G. Leuchs, Phys. Rev. A **71**, 041802(R) (2005).
[7] R. E. Slusher, L. W. Hollberg, B. Yurke, J. C. Mertz, and J. F. Valley, Phys. Rev. Lett. **55**, 2409 (1985).
[8] C. Fabre and S. Reynaud, *Quantum Noise in Optical Systems: A Semiclassical Approach*, Les Houches, Session LIII, 1990, edited by J. Dalibard, J. M. Raimond, and J. Zinn-Justin (North-Holland, Amsterdam, 1992).
[9] L. A. Wu, M. Xiao, and H. J. Kimble, J. Opt. Soc. Am. B **4**, 1465 (1987).
[10] P. D. Drummond, K. J. McNeil, and D. F. Walls, Opt. Acta **28**, 211 (1981).
[11] R. J. Glauber, Phys. Rev. **130**, 2529 (1963).
[12] C. W. Gardiner and M. J. Collett, Phys. Rev. A **31**, 3761 (1985).
[13] K. McKenzie, N. Grosse, W. P. Bowen, S. E. Whitcomb, M. B. Gray, D. E. McClelland, and P. K. Lam, Phys. Rev. Lett. **93**, 161105 (2004).
[14] P. Galatola, L. A. Lugiato, M. G. Porreca, P. Tombesi, and G. Leuchs, Opt. Commun. **85**, 95 (1991).